23rd ABCM International Congress of Mechanical Engineering
December 6-11, 2015, Rio de Janeiro, RJ, Brazil

ELIMINATION OF THE NON-PHYSICAL OSCILLATIONS IN MULTI-MATERIAL, MULTI-PHASE COMPRESSIBLE FLOWS

Saeed Parvar
Lecturer, Department of Engineering, Payam Noor University of Rasht, Iran.
S.parvar@hotmail.com
Hamid Reza Anbarlooei
Daniel .O.A. Cruz
Mechanical Engineering Program, Federal University of Rio de Janeiro (COPPE/UFRJ), Brazil
doac@mecanica.coppe.ufrj.br

Abstract. *Numerical simulation of multi material (multi-phase) flows is one of the most challenging problems among the computational fluid dynamics researches. The main difficulty of this type of the problems is the generation of unphysical oscillations at material interfaces where introduce errors into computation. For eliminating this error, a very simple algorithm proposed by Abgrall and Karni (2001) is used. Also the original 1D Cartesian model is extended to 2D axi-symmetric geometry by adding geometric source terms. Finally, using both 1D and 2D benchmark problems, the developed code is evaluated. These numerical experiments show that the results have very good accuracy in comparison with experimental and numerical result of other researches and the developed algorithm can successfully eliminate this type of error.*

Keywords: *Multi-Material Flow, Compressible Flow, Non-Physical Oscillation, Shock – Bubble Problem.*

1. INTRODUCTION

Due to advancement of the computational fluid dynamics and computational resources, researchers are trying to tackle more complex flows, especially problems involving multi-material or multi-phase compressible flows. As two or more materials interact with each other, an interface tracking algorithm is necessary to determine the location of interfaces. However it is still possible to treat such flows like single-material problems, same as "Figure 1 a.", it is more appropriate to use complex algorithms using interface tracking and mixed cells. In single material algorithm it is assumed that the interfaces are located exactly on computational grids. "Figure 1 a." shows that the location of material A with bright cells and material B with dark cells. The interface can be identified by bold dark lines which are exactly located on cells boundaries. On the other hand in multi-material algorithms, can be seen in "Figure 1 b", the interfaces usually are not located at the cell boundaries and also across the computational girds. Comparing two methods show that interfaces and multi material (mixture) cells should be considered for multi-material algorithms.

a. Single material algorithm b. Multi material algorithm

Figure 1. Comparing single material and multi material algorithm

There is a huge background on multi-material algorithms in the literature. From different problems in this field, the current paper is restricted on simple but very important one, related to generation of unphysical oscillations at material interfaces. To describe, in not properly handled multi material or multi-phase algorithms, passing any wave through material interfaces would generate unphysical oscillations which contaminate the solution. The amplitude of these oscillations is normal to wave strength, thus being critical for high speed waves, especially shock waves. Wrong calculation of fluxes at the interfaces is the reason of generating such errors (Abgrall, Karni, 2001). Fortunately, these

oscillations can be eliminated by implementing some complementary numerical algorithms. To name few, Volume of Fluid method of Nooh and Woodward (1976) , Pressure evolution model by Karni (1994), Internal energy correction algorithm ofJenny et al. (1997), and Ghost Fluid Method of Fedkiw et al. (1999) should be mentioned. Although many sophisticated algorithms had been proposed to eliminate the oscillation in the past decade, in the current research a very simple and low cost algorithm is applied to remove this error. The algorithm used here was introduced by Abgrall and Karni (2001). In addition, due to importance of axi-symmetric geometry in experimental setups, in the present work the original 1D Cartesian model is extended to 2D axi-symmetric formulations by using geometric source term.

2. GOVERNING EQUATIONS

It is well recognized that the essential mechanisms responsible for the highly nonlinear structure observed in shock waves problems can be expressed by a simple model. This model is Euler equations, where the diffusion processes are much slower than the characteristic gas-dynamic so it can be neglected. The governing (Euler) equations have the following form:

$$\frac{\partial U}{\partial t}+\frac{\partial F(U)}{\partial x}+\frac{\partial G(U)}{\partial y}=0 \tag{1}$$

$$U=\begin{bmatrix}\rho\\ \rho u\\ \rho v\\ \rho E\end{bmatrix}, F(U)=\begin{bmatrix}\rho u\\ \rho u^2+p\\ \rho uv\\ (\rho E+p)u\end{bmatrix}, G(U)=\begin{bmatrix}\rho v\\ \rho uv\\ \rho v^2+p\\ (\rho E+p)v\end{bmatrix} \tag{2}$$

here, ρ is the density, u and v are particle velocity components in the x and y directions, respectively, P is pressure, and E is the total energy per unit mass that is defined as (with the assumption that the mixture behaves like an ideal gas):

$$E=\frac{p}{\rho(\gamma-1)}+\frac{u^2+v^2}{2} \tag{3}$$

Which γ is ratio of specific heat. Ideal gas equation of state is also expressed as

$$p=\rho(\gamma-1)e \tag{4}$$

In Equation (1), U is the conservative variables vectors, and F and G are Fluxes.
An unsplit, upwind, Godunov, and 2D numerical algorithm was used in the current work. The HLLC Riemann solver is implemented for flux calculations based on Toro (2009). Also the Level set Method was implemented to track the interfaces (Osher 2002 and Sethian 1999).

2.1. Geometric Source terms

Some sophisticated problem can be simplified by taking advantage of axi-symmetric assumption. For example, in some problem which has radial symmetric, the governing equation should be rewrite in cylindrical coordinate form and then the system of equation can be treated with simpler algorithms. In the current research, to extend the Cartesian coordinate to Cylindrical situation, a very simple method was utilized by adding a geometric source term to the original Euler equation. This source term can be expressed as:

$$U_t+F(U)_z+G(U)_r=S \tag{5}$$

$$S=\begin{Bmatrix}-\frac{\alpha}{r}(\rho v)\\ -\frac{\alpha}{r}(\rho uv)\\ -\frac{\alpha}{r}(\rho v^2)\\ -\frac{\alpha}{r}((E+p)u)\end{Bmatrix} \tag{6}$$

In 2D Cartesian coordinate, α should be set equal to 1 and in 3D coordinate α should be set equal to 2 (Leveque, 2002).

2.2. Elimination of unphysical oscillatiosn

"Figure 2." shows the location on interfaces for a simple single fluid problem in 2D coordinate. Imagine two different adjacent cells have two different materials with specific primitive and conservative variable (U).

$$U_L = [\rho_L \quad \rho u_L \quad \rho v_L \quad E_L], \gamma_L, \psi_L \tag{7}$$
$$U_R = [\rho_R \quad \rho u_R \quad \rho v_R \quad E_R], \gamma_R, , \psi_R \tag{8}$$

As the flux calculation depends on these variables, any inconsistency in selecting values of these variables would lead to wrong calculation of flux. Therefore it produces unfavorable oscillations at the interfaces.

$$F_{j+\frac{1}{2}} = (U_L, U_R; \gamma_L, \gamma_R) \tag{9}$$

To solve the problem, Abgrall and Karni (2001) suggested that to calculate two different inter-cell fluxes at any material interface. First flux is computed by assuming that the both adjacent cells contain same fluid with γ_L and then second flux is computed with considering that both adjacent cells contain the other fluid with γ_R.

$$F^L_{j+\frac{1}{2}} = (U_L, U_R; \gamma_L) \tag{10}$$
$$F^R_{j+\frac{1}{2}} = (U_L, U_R; \gamma_R) \tag{11}$$

Finally, left flux ($F^L_{j+\frac{1}{2}}$) is applied to update left cell (j) variables and right flux ($F^R_{j+\frac{1}{2}}$) is used to update right cell (j+1) variables.

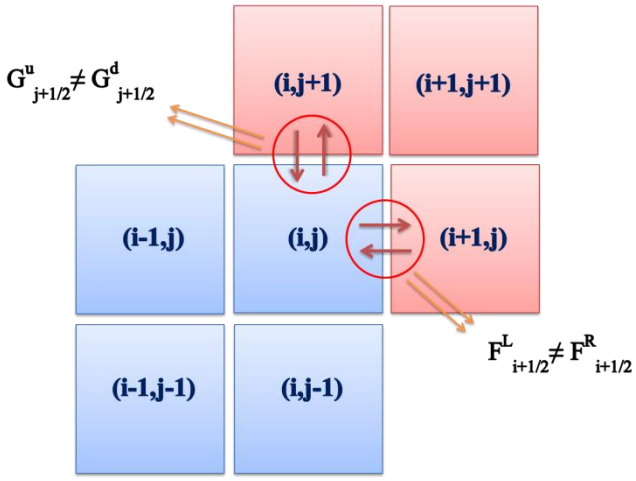

Figure 2. Schematic of developed single fluid algorithm to 2 dimensional Abgrall and karni the algorithm at the interfaces

To simplify the method, latter algorithm should be follow.

1- The Location of interface is determined by level set method.
2- Conservative variables are computed by proper equation of state.
3- If $\psi_{ij} \times \psi_{j+1} > 0$ then flux calculation is proceed like ordinary calculation so only one flux are calculated at the interfaces.
4- Else if $\psi_{ij} \times \psi_{ij+1} \leq 0$ then two different inter-cell fluxes should be calculated at the interfaces respect to γ_L or γ_R.
5- The left Flux is used to update left cell's variable and right Flux is used to update to right cell's variable.
6- New primitive variable are computed respect to their new fluxes.
7- The Same process must be done for top and down cells.
8- Level set method is computed for next step.

3. NUMERICAL RESULTS

To verifying developed algorithm two classic problems are solved in 1D coordinate. Then the code is examined for a benchmark 2D shock-bubble problem. A multi material shock bubble interaction problem was solved to check the code ability and efficiency in simulating the multi material flow in Cartesian and cylindrical coordinates.

3.1. Two material sod problem

Two material sod problem is solved without applying Abgrall and Karni's (2001) algorithm, to investigate the effect of non-physical oscillations on the results. The initial conditions can be found at "Table 1" (the variables are dimensionless).

Table 1: initial condition of two material Sod problem

Initial conditions of high pressure zone (left)	Initial conditions of low pressure zone (right)
$\begin{Bmatrix} \rho = 1.0 \\ u = 0.0 \\ p = 1.0 \\ \gamma = 1.4 \end{Bmatrix}$	$\begin{Bmatrix} \rho = 0.1 \\ u = 0.0 \\ p = 0.1 \\ \gamma = 1.6 \end{Bmatrix}$

Domain length is considered equal one and the position of diaphragm is at 0.5. One hundred cells are assumed to simulate the problem. Courant number is considered equal to 0.8 and the problem is performed till time equal to 0.2.
When diaphragm is broken, contact discontinuity moves towards right. "figure 3" shows that the motion of contact discontinuity from 0.5 to 0.67. "figure 4" displays density diagram at time=0.2, it can be seen that incorrect fluxes calculation produce unfavorable oscillation around the contact discontinuity and it moves with interfaces. The area of oscillation is specified by a red circles in the diagrams.
Non-physical fluctuations affect diagram of pressure "figure 5" and velocity "figure 6" too. There is a jump in both figures instead of smooth condition at the contact discontinuity.

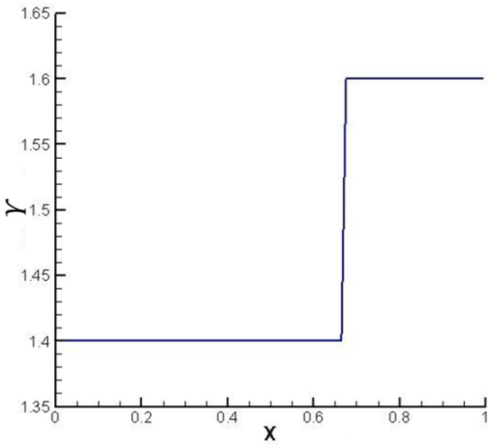

Figure 3. diagram of Gamma versus X coordinate at time=0.2

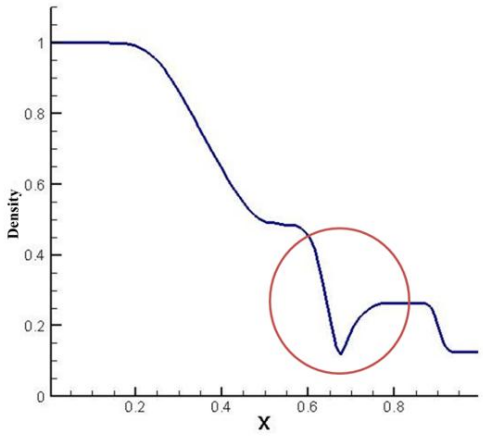

Figure 4. diagram of Density versus X coordinate at time=0.2

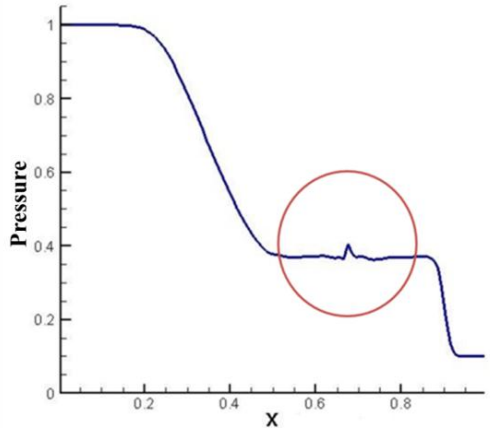

Figure 5. diagram of Pressure versus X coordinate at time=0.2

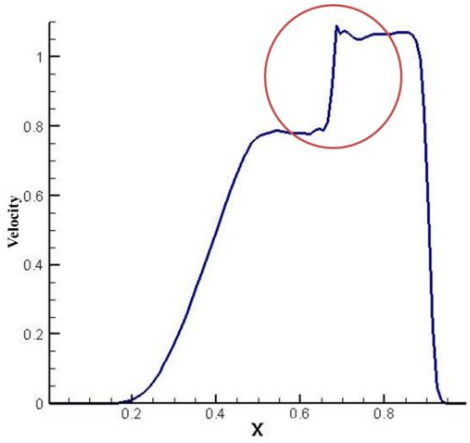

Figure 6. diagram of Velocity versus X coordinate at time=0.2

Now, Abgrall and Karni (2001) method is applied to eliminate the unfavorable oscillation at the. As it can be seen, there is no evidence of fluctuations at the interfaces for all of the curves (pressure "figure 7", density "figure 8", and velocity "figure 9"). Pressure and velocity diagrams are smooth around the contact discontinuity. It shows that the algorithm works properly and eliminates the non-physical oscillation.

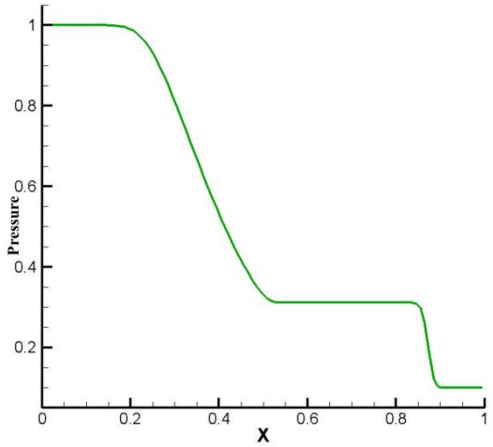

Applying Abgrall and Karni Algorithm
Figure 7. diagram of Pressure versus X coordinate at time=0.2

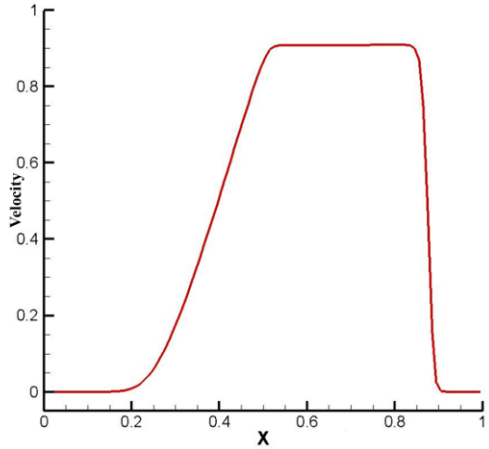

Figure 8. diagram of Velocity versus X coordinate at time=0.2

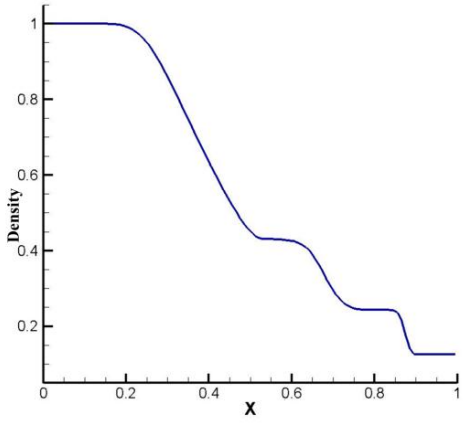

Figure 9. diagram of Density versus X coordinate at time=0.2

3.2. Two material stiff sod problem

Two material stiff sod problem is simulated to evaluate the performance of algorithm in high total energy ratio problem. The initial conditions are set equal to Table 2. Domain length is considered equal one and the position of diaphragm is at 0.5. Eight hundred cells are assumed to simulate the problem. Courant number is considered equal to 0.8 and the problem is performed till time equal to 0.01.

Table 2: initial condition of two material stiff Sod problem

Initial conditions of high pressure zone (left)	Initial conditions of low pressure zone (right)
$\begin{Bmatrix} \rho = 1.0 \\ u = 0.0 \\ p = 500.0 \\ \gamma = 1.4 \end{Bmatrix}$	$\begin{Bmatrix} \rho = 0.1 \\ u = 0.0 \\ p = 0.1 \\ \gamma = 1.6 \end{Bmatrix}$

When diaphragm is broken, shock wave and contact discontinuity move towards right. The interface position change 0.5 to 0.65 at time = 0.01. Investigating the diagrams of figure 10 prove that there is no evidence of unfavorable oscillation at the interfaces and pressure and velocity diagrams are smooth around the contact discontinuity (figure 10). In addition there are good agreement between (Abgrall, karni, 2001) result and ours.

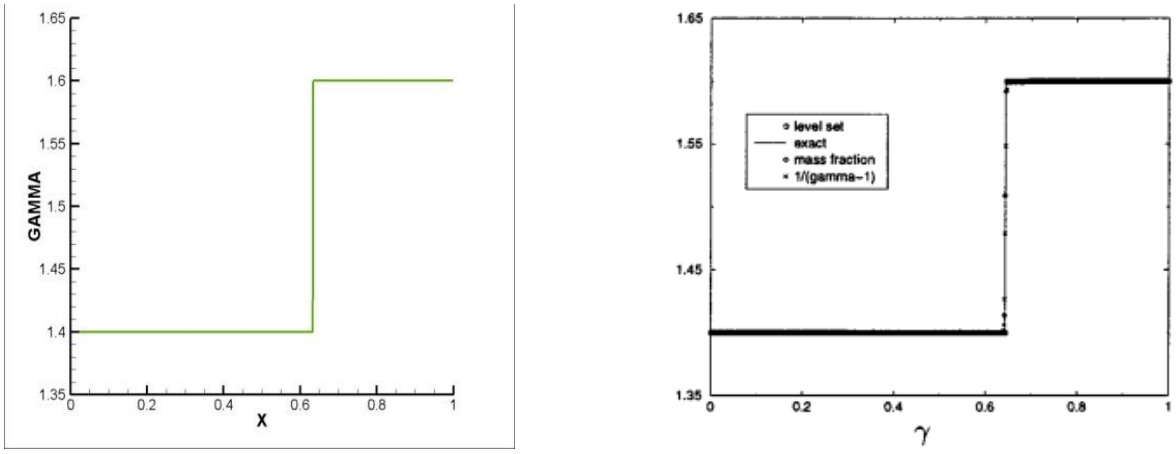

Figure 10.a. Diagram of Gamma for two material stiff sod problem at time = 0.01, Left Pictures is belong to present work and right pictures were published by (Abgrall ,Karni, 2001)

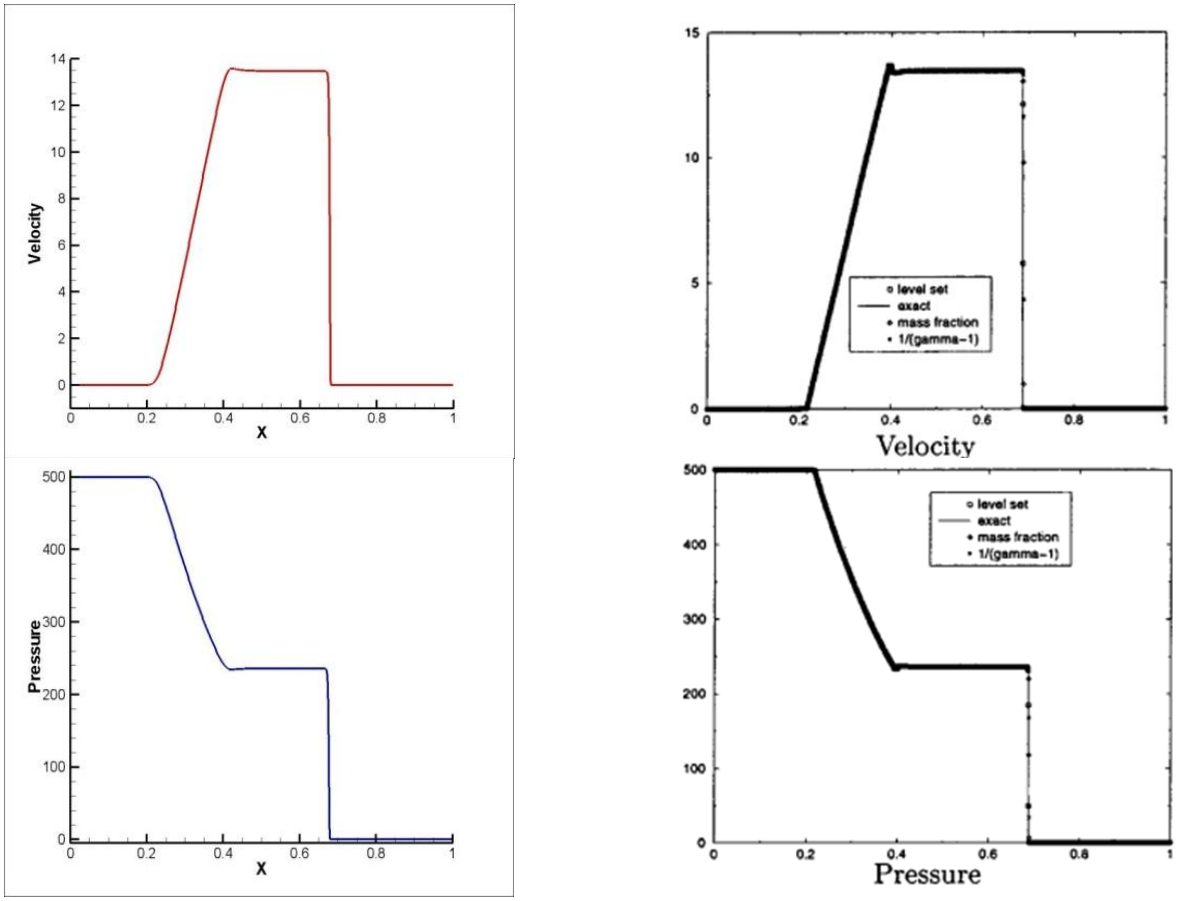

Figure 10.b. Diagram of Pressure, and Velocity for two material stiff sod problem at time = 0.01, Left Pictures is belong to present work and right pictures were published by (Abgrall, Karni ,2001)

3.2. Shock – Bubble Multi -Material Flow

Shock bubble problem is a classic and popular benchmark test for verifying numerical algorithms. To verifying developed code the standard shock –bubble (Air – Helium) interaction problem is simulated (to investigate the effect of the algorithm in 2D simulations in Cartesian and Cylindrical coordinates). At first, the problem solved in Cartesian coordinate and compared the result from Fedkiw et al. (1999) and then it solved in cylindrical coordinate and compared with experimental data. A shock wave with 1.2 Mach is assumed in X = 225 impact with a bubble with 25 unit radius which has density equal to 0.138. Center of bubble is located in X=175, Y=0. Details of the problem can be found in ("Table 3" & "Figure 11").

Table 3: Initial condition of shock – bubble problem.

$[\rho = 1 \quad u = 0 \quad v = 0 \quad p = 1 \quad \gamma = 1.4]$	Pre-Shocked air
$[\rho = 1.3764 \quad u = -0.394 \quad v = 0 \quad p = 1.5698 \quad \gamma = 1.4]$	Post-Shocked air
$[\rho = 0.138 \quad u = 0 \quad v = 0 \quad p = 1 \quad \gamma = 1.67]$	Helium

The uniform computational girds were considered equal to 650×89. When diaphragm is broken, a normal shock wave move towards left till it impacts the helium bubble. The impact of shock wave with helium bubble produce oblique shock waves which move towards the top and down walls. When oblique shock waves impact to the walls, reflects towards the center of domain. The interaction of normal shock wave and oblique shock waves with helium bubble cause formation of jet and finally results into motion and deformation of the bubble.

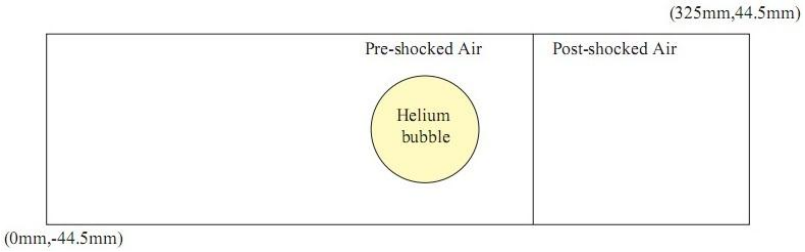

Figure 11. Schematic of Initial Condition of two material Shock Bubble Problem

"Figure 11 & 12" display contour of gamma at time = 0 and time = 427 μs. They display motion and deformation of helium bubble.

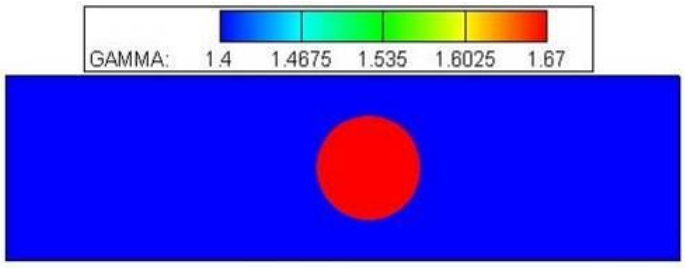

Contour of Gamma at time = 0.0

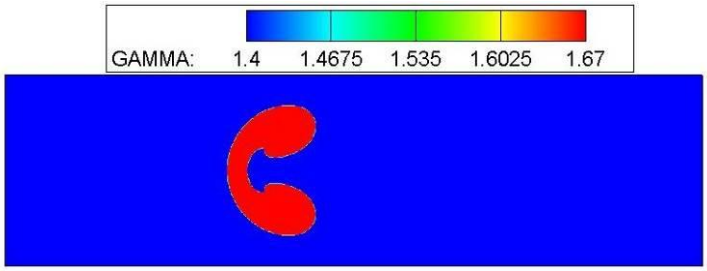

Figure 12. Contour of Gamma at time = 427. μs

Investigating the contour of pressure "figure 13" at time = 427 μs proves that there is no evidence of source and sink around the bubble. It means no non-physical oscillations are produced at the interface, so the algorithm works properly in 2D simulation too.

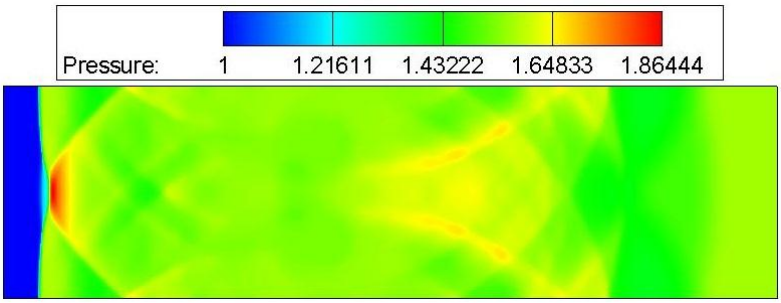

Figure.13.Contour of pressure in time = 427 μs (present work)

"Figure 14" exhibits the contour of density at time = 427 μs which can be compared with Schlieren published by Fedkiw "figure 15" (Fedkiw et al., 1999). Comparing the location of leading shock waves, oblique shock waves, and shape of helium bubble prove that there is good agreement between two results.

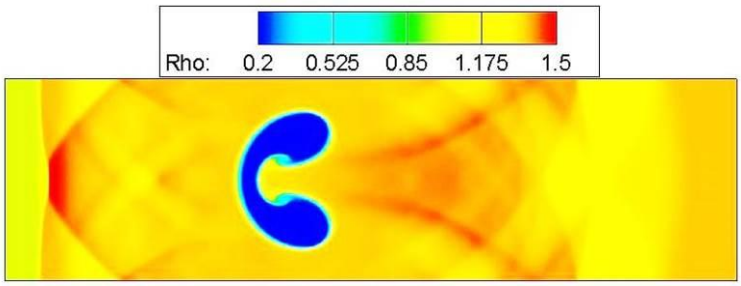

Figure.14.Contour of density in time = 427 µs (present work)

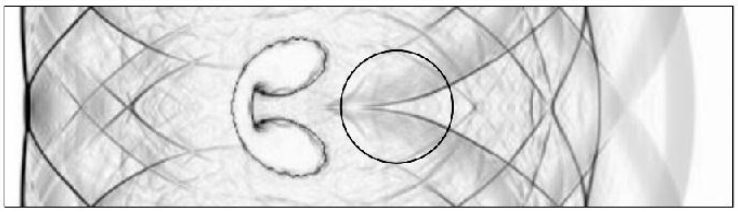

Figure.15. Schlieren of Fedkiw et al. (199) time =427 µs

To compare the result with experimental data the coordinate was changed to cylindrical by adding geometric source term "Equation 3 & 4" to the Euler equations. The shape of bubble was captured at time = 20, 223, 600 µs and then compared with Hass's reported "figures 16, 18, and 20" (Hass and Sturtevant, 1987). Non-physical oscillations have not been seen in any of results ("figures 17, 19 and 21"). Comparing the shape of bubble in three different time shows that the code results have very good accuracy and agreement in comparison with experimental data.

4. CONCLUSION

The problem of generation of the unphysical oscillations at material interfaces in multi-material flow simulations discussed. Although it is possible to use sophisticated numerical algorithms to handle this issue, a very simple, low cost, and easy to develop algorithm is examined in the current paper. The 2D and axisymmetric version of this algorithm is also developed here. The results show no evidence of the oscillation or other source of error at interfaces using this method.

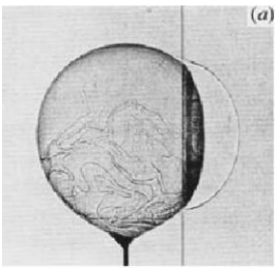

Figure.16. Schlieren from Hass and Sturtevant (1987) in time = 20 µs

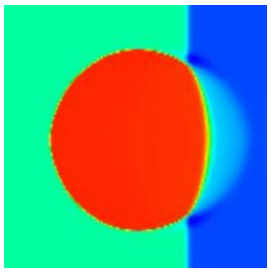

Figure.17.Contour of density in time = 20 µs

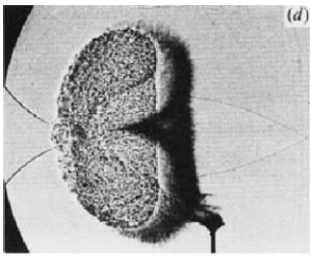

Figure.18. Schlieren from Hass and Sturtevant (1987) in time = 223 µs

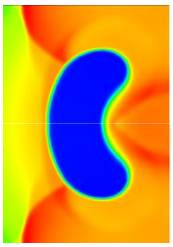

Fig.19.Contour of density in time = 223 µs

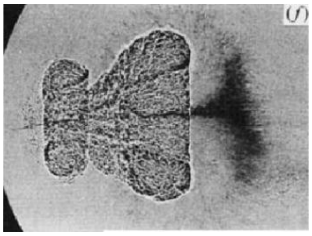

Figure.20. Schlieren from Hass and Sturtevant (1987) in time = 600 μs

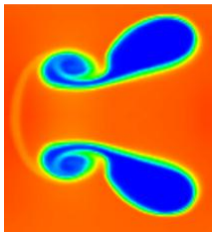

Fig.21.Contour of density in time = 600 μs

6. REFERENCES

Abgrall, R., Karni, S., "Computation of Compressible Multifluid", Journal of Computational Physics 169, pp. 594–623, 2001.

Fedkiw, R.P., Aslam, T., Merriman, B., Osher, S., "A Non-oscillatory Eulerian Approach to Interfaces in Multimaterial Flows (the Ghost Fluid Method)", Journal of Computational Physics 152, pp. 457–492 ,1999.

Jenny, P., Mueller, B., Thomann, H., 1997, "Correction of Conservative Euler Solvers for Gas Mixtures", Journal of Computational Physics, pp.132, 91.

J.F Haas , B. Sturtevant, Interaction of weak-shock waves, Journal of Fluid Mechanics, Vol. 181, pp. 41–76, 1987.

Karni, S., 1994, "Multi-component Flow Calculations by a Consistent Primitive Algorithm, Journal of Computational Physics ,pp.112, 31.

Leveque , R.J., "Finite Volume Methods for Hyperbolic Problems", Cambridge University Press, 578 pages, 2002.

Noh, W. F., Woodward, P. R. "Slic (simple line interface calculation)", in Springer Lecture Notes in Physics (Springer-Verlag, Berlin/New York), Vol. 59, pp. 330–339, 1976.

Osher, S., Fedkiw R. P.,"Level Set Methods and Dynamic Implicit Surfaces", Springer. 145, 2002.

Sethian, J.a. ,"Level Set Methods and Fast Marching Methods".: Cambridge University Press, UK, 1999.

Toro, E. F., "Riemann Solver and Numerical Method for Fluid Dynamics", Springer Press, 2009.

7. RESPONSIBILITY NOTICE

The authors are the only responsible for the printed material included in this paper.